HHS Public Access

Author manuscript

Cell Rep. Author manuscript; available in PMC 2016 May 04.

Published in final edited form as:

Cell Rep. 2016 May 3; 15(5): 926–934. doi:10.1016/j.celrep.2016.03.080.

Alternative splicing of neuronal differentiation factor TRF2 regulated by HNRNPH1/H2

Ioannis Grammatikakis[1], **Peisu Zhang**[2], **Amaresh C. Panda**[1], **Jiyoung Kim**[1], **Stuart Maudsley**[3], **Kotb Abdelmohsen**[1], **Xiaoling Yang**[1], **Jennifer L. Martindale**[1], **Omar Motiño**[1], **Emmette R. Hutchison**[2], **Mark P. Mattson**[2], and **Myriam Gorospe**[1,*]

[1]Laboratory of Genetics, National Institute on Aging-Intramural Research Program, NIH, Baltimore, MD 21224, USA

[2]Laboratory of Neurosciences, National Institute on Aging-Intramural Research Program, NIH, Baltimore, MD 21224, USA

[3]Translational Neurobiology Group, VIB Department of Molecular Genetics, University of Antwerp, Antwerpen, Belgium

SUMMARY

During neuronal differentiation, use of an alternative splice site on the rat telomere repeat-binding factor 2 (TRF2) mRNA generates a short TRF2 protein isoform (TRF2-S) capable of derepressing neuronal genes. However, the RNA-binding proteins (RBPs) controlling this splicing event are unknown. Here, using affinity pulldown analysis, we identified HNRNPH (heterogeneous nuclear ribonucleoprotein H) proteins as RBPs specifically capable of interacting with the spliced RNA segment (exon 7) of Trf2 pre-mRNA. HNRNPH proteins prevent the production of the short isoform of Trf2 mRNA, as HNRNPH silencing selectively elevates TRF2-S levels. Accordingly, HNRNPH levels decline while TRF2-S levels increase during neuronal differentiation. In addition CRISPR/Cas9-mediated deletion of hnRNPH2 selectively accelerates the NGF-triggered differentiation of rat pheochromocytoma cells into neurons. In sum, HNRNPH is a splicing regulator of Trf2 pre-mRNA that prevents the expression of TRF2-S, a factor implicated in neuronal differentiation.

Graphical abstract

*Correspondence: Laboratory of Genetics, NIA-IRP, NIH, 251 Bayview Blvd., Baltimore, MD 21224, USA, 410-558-8443, myriam-gorospe@nih.gov.

AUTHOR CONTRIBUTIONS

I.G., M.G. designed the study and interpreted the results. I.G., P.Z., A.C.P., J.K., S.M., K.A., X.Y., X.A., J.L.M., O.M., E.R.H. conducted experiments. M.P.M. contributed reagents. I.G., M.G. wrote the manuscript.

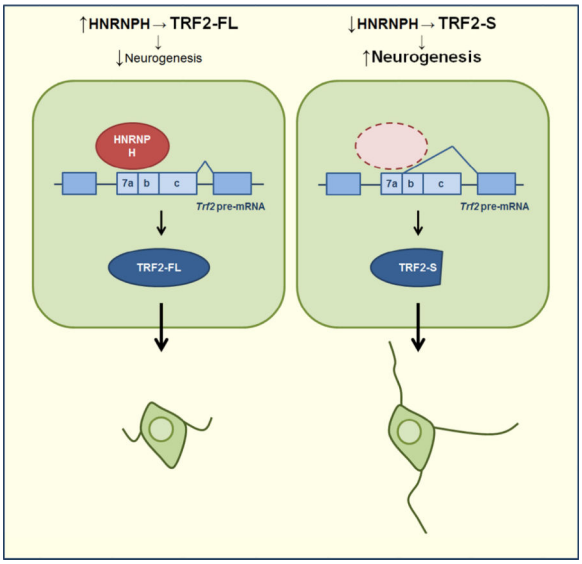

Keywords

TRF2; TRF2-S; HNRNPH; alternative splicing; mRNA; ribonucleoprotein complex

INTRODUCTION

The protein telomeric repeat-binding factor 2 (TRF2, also known as TERF2 and TRBF2) was originally identified as part of a protein complex named shelterin that protects telomeres, the regions at the ends of chromosomes (de Lange, 2005). Extra-telomeric functions for TRF2 have also emerged recently. In differentiating human embryonic stem cells, increased TRF2 levels promotes the expression of REST (repressor element-1 silencing transcription factor), a negative regulator of neuronal genes; conversely, TRF2 inhibition in rodents promotes neuronal differentiation (Schoenherr and Anderson, 1995; Ovando-Roche et al., 2014). A dominant negative form of TRF2 triggered a DNA damage response and senescence in mitotic neural cells, while TRF2 inhibition enhanced differentiation of hippocampal neurons (Zhang et al., 2006). TRF2 binds to REST and protects it from proteasomal degradation, causing repression of neuronal genes and inhibition of neuronal differentiation (Zhang et al., 2008). In rodents, TRF2 inhibition promoted neuronal differentiation, while TRF2 depletion in patient glioblastoma stem cells reduced cell proliferation and increased expression of proteins targeted for repression by REST (Bai et al., 2014).

The gene that encodes TRF2 contains 10 exons and is subject to alternative splicing. Recently, a new isoform of TRF2 was identified, TRF2-S; in rodents, TRF2-S arises when a 5’ alternative splice site on exon 7 is used and only part of exon 7 (exon 7a) in *Trf2* pre-mRNA is included in the mature *Trf2* mRNA (Zhang et al., 2011). The resulting protein isoform lacks the DNA-binding domain and nuclear localization signal (NLS) and instead possesses a short sequence that retains TRF2-S in the cytoplasm. TRF2-S maintains the

ability to bind to REST and renders it inactive in the cytoplasm, in turn derepressing neuronal genes and inducing differentiation of rat cortical neurons (Zhang et al., 2011).

The spliceosome catalyzes exon joining and intron removal as pre-mRNAs are processed into mature mRNAs (Wahl et al., 2009). The vast majority of human genes that contain more than one exon undergo alternative splicing with variable expression among tissues (Wang et al., 2008). Alternative splicing is a major contributor to protein isoform diversity, since a single precursor mRNA can give rise to multiple mRNA splice variants (Cooper, 2005) depending on pre-mRNA sequences that act as *cis*-acting elements around splice sites (Barash et al., 2010). RNA-binding proteins (RBPs) that function as alternative splicing regulators bind to pre-mRNA *cis*-acting elements and can promote or repress spliceosome formation and thus regulate alternative splice site usage in the mature transcript (Blencowe, 2006).

Previous studies have identified alternative splicing regulators in neurons (Calarco et al., 2011), but the RBPs involved in regulating TRF2 splicing and hence neuronal differentiation are unknown. Here, through a proteomic screen we identified RBPs interacting with exon 7 of the *Trf2* pre-mRNA. Two RBPs of the heterogeneous nuclear ribonucleoprotein H (HNRNPH) family were capable of binding and inhibiting the use of the 5' alternative splice site on exon 7, promoting inclusion of exon 7 of *Trf2* pre-mRNA, and thereby increasing the relative levels of full-length (FL) TRF2 and lowering TRF2-S abundance. CRISPR-mediated reduction of HNRNPH accelerated neuronal differentiation, suggesting a critical role for HNRNPH as repressor of neurogenesis.

RESULTS

Proteomic screen to identify HNRNPH among the proteins binding to *Trf2* exon 7 RNA

TRF2-S is a short isoform of protein TRF2 that is produced when an alternative 5' splice site of exon 7 is used and a shorter segment of exon 7 is spliced into the mature *Trf2* mRNA (Fig. 1A) (Zhang et al., 2011). A premature termination codon is then created that produces TRF2-S (330-amino acids (aa) long), shorter than the ~500-aa long full-length TRF2. TRF2-S can still bind REST and renders REST inactive in the cytoplasm, leading to neuronal gene derepression and neuronal differentiation.

We sought to identify the RBPs controlling TRF2 5' alternative splice site use and hence TRF2-S production. A ~1-kb PCR product from rat genomic DNA containing exon 7 plus flanking sequences (~300 nt in each direction, Fig. 1B) was used as a template for *in vitro* transcription of biotinylated RNA. Nuclear extracts prepared from rat cerebellum and kidney (a control tissue) were used for identifying RBPs binding to the biotinylated RNA; a negative control RNA [biotinylated rat *Gapdh* 3'-untranslated region (UTR)] was included. The ~80 proteins selectively bound to biotinylated *Trf2* RNA (Table S1) were further selected as explained (supplemental text). They included several RBPs [e.g., ELAVL1 (HuR), ELAVL3 (HuC), RBM14, and RNA helicases DDX17 and DDX5] and hnRNPs HNRNPH1 and HNRNPH2, which were shown to modulate alternative splicing (Huelga et al., 2012; Katz et al., 2010; Stark et al., 2011; Turunen et al., 2013; Uren et al., 2016), HNRNPF, HNRNPA3 and HNRNPD0. HNRNPF is functionally related to the HNRNPH

family and was shown to regulate splicing (Mandler et al., 2014; Wang et al., 2012). Other RBPs identified in kidney extracts included Staufen 1 (STAU1) and the splicing regulator polypyrimidine tract-binding protein 1 (PTB) (Boutz et al., 2007; Li et al., 2014). In summary, we identified RBPs selectively binding to *Trf2* exon 7 RNA in rat cerebellar extracts (Fig. 1C).

Fourteen RBPs that interacted selectively with *Trf2* exon 7 RNA and might have a role in neuronal gene regulation were studied for their influence on TRF2 alternative splicing using an *ex vivo* functional splicing assay that employed the RNA sequence used in the RNA affinity pulldown assay (Fig. 1B) cloned into a minigene (Fig. 1D, *top*). After transient transfection of rat pheochromocytoma PC12 cells with small interfering (si)RNAs directed at each RBP, the degree of knockdown achieved was measured 48 h later by reverse transcription (RT) followed by real-time, quantitative (q)PCR analysis of each RBP mRNA (Fig. 1D, *lower*). The effect of each knockdown was then assayed on *Trf2* pre-mRNA splicing by RT followed by semi-quantitative PCR analysis using primers directed at the flanking exons ('minigene'); similar primers were used to assay endogenous *Trf2* transcripts spanning exon 7a and exon 8 ('endogenous') (Fig. 1E–G). Besides *Trf2-FL* and *Trf2-S* (observed at the expected sizes), an intermediate-sized band was observed that potentially corresponds to *Trf2-S'* (Zhang et al., 2011). As shown, the ratio of the *Trf2-FL* and *Trf2-S* isoform in the minigene and endogenous transcript assays did not change significantly for the siRNAs tested, except when HNRNPH1 or H2 were knocked down, while HNRNPF did not have any effect on *Trf2* splicing (Fig. 1E–G). These results indicate that HNRNPH proteins can potentially regulate TRF2 alternative splicing.

HNRNPH1 and HNRNPH2 are >95% identical paralogs of the HNRNPH RBP family. To test if they might influence splicing in similar ways, we used two different siRNAs directed at each HNRNPH. As shown (Fig. 1H–J), by 48 h after transfection, all siRNAs lowered HNRNPH and shifted the ratio of *Trf2* towards the production of less *Trf2-FL* mRNA and more *Trf2-S* mRNA (endogenous and minigene). Less efficient HNRNPH2 knockdown led to more modest *Trf2* splicing, while HNRNPH1 silencing lowered both H1 and H2, possibly explaining why H1 siRNA more strongly favored splicing of *Trf2-S* (Fig. 1H–K).

HNRNPH binds *Trf2* pre-mRNA, inhibits splicing of exon 7, and lowers TRF2-S production

Given earlier evidence that HNRNPH associated with biotinylated *Trf2* RNA exon 7, we performed RIP [ribonucleoprotein (RNP) immunoprecipitation (IP)] analysis to investigate this interaction further. HNRNPH was immunoprecipitated from PC12 cell extracts and its interaction with *Trf2* RNA was measured by RT-qPCR analysis employing two different sets of primers (Fig. 2A). This interaction was measured as the enrichment in *Trf2* RNA in HNRNPH IP compared with IgG IP; the levels of *Tbp* mRNA, encoding a housekeeping protein, in each IP were used to normalize differences in sample input. We then tested if HNRNPH contributed to the use of the alternative splice site of *Trf2* pre-mRNA into protein; Western blot analysis with an antibody that recognized both isoforms revealed that TRF2-S levels were higher and TRF2-FL lower after silencing either HNRNPH1 or HNRNPH2 (Fig. 2B,C). Measurement of *Trf2-FL* and *Trf2-S* mRNAs on polysome gradients indicated that HNRNPH2 silencing did not influence the translation of either protein isoform (not shown).

In addition, actinomycin D treatment of PC12 cells after silencing HNRNPH showed that HNRNPH did not affect *Trf2-S* or *Trf2-FL* mRNA stability (Fig. S1). Collectively, these results suggest that HNRNPH inhibits the use of an alternative splice site on exon 7 and the production of the short transcript (*Trf2-S*) and favors production of the longer transcript (*Trf2-FL*); accordingly, HNRNPH silencing induced TRF2-S protein production.

To map the site of interaction of HNRNPH with *Trf2* pre-mRNA, the region surrounding exon 7 was divided into 7 overlapping fragments, each ~150 nt in length (Fig. 2D, *top*). Biotin pulldown analysis using whole-cell extracts from PC12 cells showed that HNRNPH associated with fragments 2 and 4 (Fig. 2D, *bottom*); further subdivision of these RNAs into 30-nt fragments showed that F2-5, F4-4, and F4-5 contained binding sequences for HNRNPH (Fig. 2E). Previous studies characterized the binding sequence of HRNPH1 as 5- to 8-nt long sequence rich in Gs and As (Huelga et al., 2012; Uren et al., 2016). When sequences F2-5, F4-4, and F4-5 were mutated into stretches of Us, biotin pulldown showed that binding was abolished (Fig. 2F). In all assays, negative controls (biotinylated rat *Gapdh* 3'UTR and beads only) were included (Fig. 2D–F).

We then examined whether these binding sites influenced the use of an alternative splice site by HNRNPH. We inserted the same mutations that abolish binding (Fig. 2F) into the minigenes that were used as *Trf2* splicing reporters (Fig. 1) and conducted splicing assays after transfection of PC12 cells along with scrambled siRNA, siRNAs directed at HNRNPH1 or H2. As shown (Fig. 2G), knockdown of either HNRNPH1 or H2 lowered *Trf2-FL* and elevated *Trf2-S*, suggesting that all three binding sites may regulate HNRNPH binding and *Trf2* splicing. The minigene with the mutated F4-4 sequence showed lower basal level of inclusion (Scrambled siRNA), indicating that this site may have a stronger effect on HNRNPH regulation of *Trf2* splicing, while for the minigene with mutated F4-5 sequence, the basal levels of inclusion increased, likely because a *cis*-element promoting *Trf2-S* was disrupted by the mutation. Collectively, these results indicate that HNRNPH can bind to three distinct binding sites near or on exon 7 and potentially all of them play a role in regulation of *Trf2* splicing.

HNRNPH levels decrease during neuronal differentiation

TRF2-S was recently shown to play a role in neuronal differentiation. Since TRF2-S contributes to REST inactivation and rat cortical neuron differentiation, a factor that regulates TRF2-S abundance may also coordinate neuronal differentiation. To test if HNRNPH plays a role in this process, we examined HNRNPH expression levels at different times during differentiation of rat cortical neurons. We observed a gradual decrease in the levels of HNRNPH (Fig. 3A), in the absence of comparable changes in *Hnrnph1* and *Hnrnph2* mRNAs (Fig. 3B, *top*); at the same time, there was a gradual increase in TRF2-S protein, as reported earlier (Zhang et al., 2011) and decrease in TRF2-FL (Fig. 3A). A gradual increase of *Trf2-S* mRNA and decrease of *Trf2-FL* mRNA was also observed (Fig. 3B, *bottom*).

In another model of neuronal differentiation, treatment of PC12 cells with NGF in the presence of low serum triggers their differentiation into neurons in 7–10 days, with formation of neurites (Das et al., 2004). Here too, during NGF-triggered differentiation,

HNRNPH levels decreased gradually (Fig. 3C), *Hnrnph1* and *Hnrnph2* mRNAs decreased only moderately, and there was a gradual increase of *Trf2-S* and decrease of *Trf2-FL* (Fig. 3D). These findings indicate that HNRNPH proteins are downregulated during rat neuronal differentiation and suggest an inhibitory role for HNRNPH in this process.

HNRNPH regulates neuronal differentiation

Several RBPs have been linked to neuronal differentiation (Calarco et al., 2011; Grabowski, 2011). Since HNRNPH inhibits TRF2-S production and HNRNPH levels decrease during differentiation, we hypothesized that HNRNPH may have an inhibitory influence on neuronal differentiation. To investigate this possibility, we reduced HNRNPH2 levels and studied if neuronal differentiation progressed at a different rate. HNRNPH siRNA transfections were transient and thus unable to maintain reduced HNRNPH levels for extended time periods (not shown). Therefore, CRISPR technology was employed to lower HNRNPH2 levels. PC12 cells expressing Cas9 and guide (g)RNA targeting *Hnrnph2* were generated by lentiviral infection. The transduced cells expressed a puromycin resistance gene for selection and a GFP reporter gene for identification of cells expressing the transgene (Fig. 4A). Western blot analysis confirmed the downregulation of HNRNPH and the switch in the ratio of TRF2-FL and TRF2-S levels (Fig. 4B); RT-qPCR analysis verified the decline in *Hnrnph2* mRNA levels (Fig. 4C, *top*) and the change in the *Trf2-S* and *Trf2-FL* mRNA levels (Fig. 4C, *bottom*). After treating the cells with differentiation media, cells with reduced HNRNPH2 levels showed accelerated differentiation relative to control cells; these changes were observed at different days, including day 6 (Fig. 4D). Differentiated cells were counted if there was at least one neurite extension that was at least twice the diameter of the cell body. As shown, significantly more cells differentiated in the CRISPR-HNRNPH2 populations (Fig. 4E). Analysis of clonal populations (Fig. S2A) showed that differentiation was consistently accelerated in cells with reduced HNRNPH2 than in control cells. Finally, the importance of HNRNPH in neuronal differentiation is supported by the fact that HNRNPH levels are much higher in rat cortex than in rat liver or kidney (Fig. S2B,C). Collectively, these data support the hypothesis that HNRNPH inhibits neuronal differentiation.

DISCUSSION

Alternative splicing is a major contributor to protein isoform diversity and explains the fact that the number of human genes is much lower than the number of distinct proteins expressed in a given cell (Nilsen and Graveley, 2010). Here, we identified HNRNPH as a regulator of *Trf2* alternative splicing that inhibits the production of the shorter protein isoform, TRF2-S. The consequences of this regulation were studied in two models of neuronal differentiation: rat PC12 cells treated with NGF and neurogenesis of rat primary cortical neurons. In both systems, differentiation triggered a gradual decrease of HNRNPH levels concomitant with an increase in *Trf2-S*. Importantly, inhibition of HNRNPH2 in PC12 cells using CRISPR accelerated neuronal differentiation.

Previous studies have identified several alternative splicing regulators implicated in neuronal cell differentiation (Calarco et al., 2011). A characteristic example is the neuronal-specific

RBP NOVA, which binds RNA (Licatalosi et al., 2008; Ule et al., 2006) and regulates splicing of genes encoding synaptic proteins (Irimia et al., 2011; Zhang et al., 2010). During neuronal differentiation, reprogramming of alternative splicing events depends on the switch on the expression of PTB to the isoform nPTB, that is neuronal specific (Boutz et al., 2007). This switch is responsible for reprogramming a network of alternative splicing events in the developing neurons implicated in neuronal maturation (Boutz et al., 2007; Li et al., 2014). Another RBP, nSR100, regulates brain-specific alternative exons enriched in genes related to neural differentiation and its inhibition disrupts neural cell differentiation in culture in developing zebrafish (Calarco et al., 2009).

The splicing regulator involved in neuronal differentiation described here, HNRNPH, belongs to a family of hnRNPs originally identified to regulate splicing (Martinez-Contreras et al., 2007) that contain RRM or KH RNA-binding domains. Several high-throughput studies have characterized the role of HRNPH1 in splicing, mRNA stability and polyadenylation (Huelga et al., 2012; Katz et al., 2010; Uren et al., 2016; Wang et al., 2012). The most recent of these studies identified a CLIP tag on the human homolog of *Trf2* (Uren et al., 2016) and identified potential binding sites as G tracts containing As (Huelga et al., 2012; Uren et al., 2016). HNRNPH1 was previously shown to regulate alternative splicing in oligodendrocytes (Mandler et al., 2014; Wang et al., 2012) and exon inclusion of several transcripts encoding brain-specific proteins C1 cassette exon of the glutamate NMDA R1 receptor (GRIN1) mRNA (Han et al., 2005), and was proposed to promote c-Src N1 exon inclusion in neuronal cells (Chou et al., 1999) and exon 2 inclusion on the OPRM1 (μ opioid receptor) (Xu et al., 2014). REST is also regulated via alternative splicing (Chen and Miller, 2013); interestingly, HNRNPH1 regulates the neuronal-specific exon N of REST in H69 small-cell lung cancer cells and is a pre-requisite for binding of the splicing factor U2AF65 and subsequent exon inclusion (Ortuno-Pineda et al., 2012). Together with our findings, these studies underscore the importance of HNRNPH1 in controlling alternative splicing of neural genes.

By contrast, the paralog HNRNPH2 has not been studied extensively. Its role in alternative splicing was previously described for thymidine phosphorylase (TP), where binding of HNRNPH2 to the *TP* pre-mRNA caused intron retention and repression of TP translation leading to anti-cancer drug resistance due to loss of TP (Stark et al., 2011). In addition, HNRNPH2 was shown to interact with CUG repeats, implicated in Myotonic Dystrophy (DM), and was later identified as a regulator of exon 11 of the insulin receptor gene, an alternative splicing event is that is misregulated in DM (Paul et al., 2011). While this study implicates HNRNPH1 in neuronal differentiation, its functions may overlap with those of HNRNPH2, since the two proteins are >95% identical. As shown, the U12-dependent spliceosome component U11-48K is regulated by binding of HNRNPH1 and HNRNPH2 to a stretch of Gs of the *U11-48K* pre-mRNA to induce skipping of exon 4i and protect the mRNA from nonsense-mediated decay (NMD) (Turunen et al., 2013).

The binding sites for HNRNPH on near exon 7 were identified experimentally (Fig. 2) and guided by previous studies (Huelga et al., 2012; Uren et al., 2016). Mutating the sites into stretches of Us abolished binding, even though it did not fully abolish splicing, suggesting that there are additional sites through which HNRNPH regulates splicing, that the three sites

are partially redundant, or that HNRNPH does not inhibit the use of the alternative splice site but rather promotes the use of the downstream site. Multiple simultaneous disruptions of HNRNPH sites on the minigene were not tested, as excessive modification of the splicing site would have rendered the splicing data inconclusive. In addition, while HNRNPH regulation on splicing was linked to the closely related protein HNRNPF (Mandler et al., 2014; Wang et al., 2012), HNRNPF had no effect on *Trf2* splicing (Fig. 1); whether the two proteins synergize in this context was not examined.

Both paralogs control splicing of *Trf2-S*, although HNRNPH1 appeared to have a stronger splicing effect in suppressing TRF2-S. Unexpectedly, CRISPR/Cas9 successfully downregulated HNRNPH2, but did not yield any clones in which HNRNPH1 was downregulated, despite numerous attempts. Perhaps cells with efficient HNRNPH1 downregulation may differentiate spontaneously and thus stop dividing, precluding clonal expansion. HNRNPH protein levels were profoundly downregulated while *Hnrnph1* and *Hnrnph2* mRNAs were not (Fig. 3) and did not appear to be subject to altered turnover (Fig. S1), despite the presence of a premature termination codon in exon 8 of the shorter isoform of *Trf2* (Zhang et al., 2011) which might trigger NMD. These findings led us to propose that HNRNPH protein levels in neuronal tissues are tightly regulated at the level of translation or protein stability. Possibly for these reasons our attempts to overexpress HNRNPH were also unsuccessful (not shown).

In sum, we have identified HNRNPH as a factor that represses neuronal differentiation at least in part by inhibiting the alternative splicing of TRF2 into the pro-differentiation isoform TRF2-S. Given that almost certainly other RNA targets of HNRNPH also contribute to preventing neuronal differentiation, identifying these additional effectors is warranted, whether HNRNPH influences splicing or other post-transcriptional processes. Conversely, other splicing factors that our screen may have missed may also cooperate with HNRNPH to regulate TRF2 splicing. Further studies employing the approaches outlined here will help us understand comprehensively the impact of HNRNPH and TRF2 upon neuronal differentiation.

EXPERIMENTAL PROCEDURES

RNA analysis

The oligomers and conditions used for *in vitro* transcription, preparation of biotinylated RNA, and RNA pulldown assays are indicated in SI Methods. The minigene cloning and splicing assay were carried out as described (Singh and Cooper, 2006) using the primers listed in Table S2. Ribonucleoprotein immunoprecipitation (RIP) analysis were carried out as reported earlier (Abdelmohsen et al., 2012), and reverse transcription (RT) followed by conventional PCR and by real-time quantitative (q)PCR analyses are explained (supplemental text).

Protein analysis

The preparation of cerebellum and kidney extracts, as well as the mass spectrometry details are in SI Methods. Western blot analysis was performed using standard methods, and protein signals were detected using the antibodies listed (supplemental text).

Cell culture, differentiation, transfection, and CRISPR/Cas9

Rat cortical neurons were extracted from rat embryos on E17 as described previously (Zhang et al., 2011) and PC12 cells were cultured as explained in the supplemental text. Transfections were carried out using polyethylenimine (Sigma Aldrich) (PEI) and Lipofectamine; siRNA sequences directed at different proteins are listed in Table S3.

To study differentiation of primary neurons, neurobasal media containing B27 supplement (Gibco, Carlsbad, CA, USA) was used. To generate stable PC12 cells, we used a CRISPR/Cas9 vector (Sigma Aldrich) targeting the sequence ACTTTCAGGGGCGGAGCACAGG.

Statistical analysis

Data are presented as means ± SEM. Significance was tested using two-tailed Student's t test. $p<0.05$ was considered significant.

Supplementary Material

Refer to Web version on PubMed Central for supplementary material.

Acknowledgments

This work was supported in its entirety by the NIA-IRP, NIH.

REFERENCES

Abdelmohsen K, Tominaga-Yamanaka K, Srikantan S, Yoon JH, Kang MJ, Gorospe M. RNA-binding protein AUF1 represses Dicer expression. Nucleic Acids Res. 2012; 40:11531–11544. [PubMed: 23066106]

Bai Y, Lathia JD, Zhang P, Flavahan W, Rich JN, Mattson MP. Molecular targeting of TRF2 suppresses the growth and tumorigenesis of glioblastoma stem cells. Glia. 2014; 62:1687–1698. [PubMed: 24909307]

Barash Y, Calarco JA, Gao W, Pan Q, Wang X, Shai O, Blencowe BJ, Frey BJ. Deciphering the splicing code. Nature. 2010; 465:53–59. [PubMed: 20445623]

Blencowe BJ. Alternative splicing: new insights from global analyses. Cell. 2006; 126:37–47. [PubMed: 16839875]

Boutz PL, Stoilov P, Li Q, Lin CH, Chawla G, Ostrow K, Shiue L, Ares M Jr, Black DL. A post-transcriptional regulatory switch in polypyrimidine tract-binding proteins reprograms alternative splicing in developing neurons. Genes Dev. 2007; 21:1636–1652. [PubMed: 17606642]

Calarco JA, Superina S, O'Hanlon D, Gabut M, Raj B, Pan Q, Skalska U, Clarke L, Gelinas D, van der Kooy D, et al. Regulation of vertebrate nervous system alternative splicing and development by an SR-related protein. Cell. 2009; 138:898–910. [PubMed: 19737518]

Calarco JA, Zhen M, Blencowe BJ. Networking in a global world: establishing functional connections between neural splicing regulators and their target transcripts. RNA. 2011; 17:775–791. [PubMed: 21415141]

Chen GL, Miller GM. Extensive alternative splicing of the repressor element silencing transcription factor linked to cancer. PLoS ONE. 2013; 8:e62217. [PubMed: 23614038]

Chou MY, Rooke N, Turck CW, Black DL. hnRNP H is a component of a splicing enhancer complex that activates a c-src alternative exon in neuronal cells. Mol. Cell. Biol. 1999; 19:69–77. [PubMed: 9858532]

Cooper TA. Use of minigene systems to dissect alternative splicing elements. Methods. 2005; 37:331–340. [PubMed: 16314262]

Das KP, Freudenrich TM, Mundy WR. Assessment of PC12 cell differentiation and neurite growth: a comparison of morphological and neurochemical measures. Neurotoxicol. Teratol. 2004; 26:397–406. [PubMed: 15113601]

de Lange T. Shelterin: the protein complex that shapes and safeguards human telomeres. Genes Dev. 2005; 19:2100–2110. [PubMed: 16166375]

Grabowski P. Alternative splicing takes shape during neuronal development. Curr. Op. Genet. Dev. 2011; 21:388–394. [PubMed: 21511457]

Han K, Yeo G, An P, Burge CB, Grabowski PJ. A combinatorial code for splicing silencing: UAGG and GGGG motifs. PLoS Biol. 2005; 3:e158. [PubMed: 15828859]

Huelga SC, Vu AQ, Arnold JD, Liang TY, Liu PP, Yan BY, Donohue JP, Shiue L, Hoon S, Brenner S, et al. Integrative genome-wide analysis reveals cooperative regulation of alternative splicing by hnRNP proteins. Cell Rep. 2012; 1:167–178. [PubMed: 22574288]

Irimia M, Denuc A, Burguera D, Somorjai I, Martin-Duran JM, Genikhovich G, Jimenez-Delgado S, Technau U, Roy SW, Marfany G, et al. Stepwise assembly of the Nova-regulated alternative splicing network in the vertebrate brain. Proc. Natl. Acad. Sci. USA. 2011; 108:5319–5324. [PubMed: 21389270]

Katz Y, Wang ET, Airoldi EM, Burge CB. Analysis and design of RNA sequencing experiments for identifying isoform regulation. Nat. Methods. 2010; 7:1009–1015. [PubMed: 21057496]

Kim YK, Furic L, Parisien M, Major F, DesGroseillers L, Maquat LE. Staufen1 regulates diverse classes of mammalian transcripts. EMBO J. 2007; 26:2670–2681. [PubMed: 17510634]

Li Q, Zheng S, Han A, Lin CH, Stoilov P, Fu XD, Black DL. The splicing regulator PTBP2 controls a program of embryonic splicing required for neuronal maturation. eLife. 2014; 3:e01201. [PubMed: 24448406]

Licatalosi DD, Mele A, Fak JJ, Ule J, Kayikci M, Chi SW, Clark TA, Schweitzer AC, Blume JE, Wang X, et al. HITS-CLIP yields genome-wide insights into brain alternative RNA processing. Nature. 2008; 456:464–469. [PubMed: 18978773]

Mandler MD, Ku L, Feng Y. A cytoplasmic quaking I isoform regulates the hnRNP F/H-dependent alternative splicing pathway in myelinating glia. Nuc. Acids Res. 2014; 42:7319–7329.

Martinez-Contreras R, Cloutier P, Shkreta L, Fisette JF, Revil T, Chabot B. hnRNP proteins and splicing control. Adv. Exp. Med. Biol. 2007; 623:123–147. [PubMed: 18380344]

Nilsen TW, Graveley BR. Expansion of the eukaryotic proteome by alternative splicing. Nature. 2010; 463:457–463. [PubMed: 20110989]

Ortuno-Pineda C, Galindo-Rosales JM, Calderon-Salinas JV, Villegas-Sepulveda N, Saucedo-Cardenas O, De Nova-Ocampo M, Valdes J. Binding of hnRNP H and U2AF65 to respective G-codes and a poly-uridine tract collaborate in the N50-5'ss selection of the REST N exon in H69 cells. PLoS ONE. 2012; 7:e40315. [PubMed: 22792276]

Ovando-Roche P, Yu JS, Testori S, Ho C, Cui W. TRF2-mediated stabilization of hREST4 is critical for the differentiation and maintenance of neural progenitors. Stem Cells. 2014

Paul S, Dansithong W, Jog SP, Holt I, Mittal S, Brook JD, Morris GE, Comai L, Reddy S. Expanded CUG repeats Dysregulate RNA splicing by altering the stoichiometry of the muscleblind 1 complex. J. Biol. Chem. 2011; 286:38427–38438. [PubMed: 21900255]

Schoenherr CJ, Anderson DJ. The neuron-restrictive silencer factor (NRSF): a coordinate repressor of multiple neuron-specific genes. Science. 1995; 267:1360–1363. [PubMed: 7871435]

Singh G, Cooper TA. Minigene reporter for identification and analysis of cis elements and trans factors affecting pre-mRNA splicing. Biotechniques. 2006; 41:177–181. [PubMed: 16925019]

Stark M, Bram EE, Akerman M, Mandel-Gutfreund Y, Assaraf YG. Heterogeneous nuclear ribonucleoprotein H1/H2-dependent unsplicing of thymidine phosphorylase results in anticancer drug resistance. J. Biol. Chem. 2011; 286:3741–3754. [PubMed: 21068389]

Turunen JJ, Verma B, Nyman TA, Frilander MJ. HnRNPH1/H2, U1 snRNP, and U11 snRNP cooperate to regulate the stability of the U11-48K pre-mRNA. RNA. 2013; 19:380–389. [PubMed: 23335637]

Ule J, Stefani G, Mele A, Ruggiu M, Wang X, Taneri B, Gaasterland T, Blencowe BJ, Darnell RB. An RNA map predicting Nova-dependent splicing regulation. Nature. 2006; 444:580–586. [PubMed: 17065982]

Uren PJ, Bahrami-Samani E, de Araujo PR, Vogel C, Qiao M, Burns SC, Smith AD, Penalva LO. High-throughput analyses of hnRNP H1 dissects its multi-functional aspect. RNA Biol. 2016 [Epub ahead of print].

Wahl MC, Will CL, Luhrmann R. The spliceosome: design principles of a dynamic RNP machine. Cell. 2009; 136:701–718. [PubMed: 19239890]

Wang ET, Sandberg R, Luo S, Khrebtukova I, Zhang L, Mayr C, Kingsmore SF, Schroth GP, Burge CB. Alternative isoform regulation in human tissue transcriptomes. Nature. 2008; 456:470–476. [PubMed: 18978772]

Wang E, Aslanzadeh V, Papa F, Zhu H, de la Grange P, Cambi F. Global profiling of alternative splicing events and gene expression regulated by hnRNPH/F. PLoS ONE. 2012; 7:e51266. [PubMed: 23284676]

Wang E, Dimova N, Cambi F. PLP/DM20 ratio is regulated by hnRNPH and F and a novel G-rich enhancer in oligodendrocytes. Nuc. Acids Res. 2007; 35:4164–4178.

Xu J, Lu Z, Xu M, Pan L, Deng Y, Xie X, Liu H, Ding S, Hurd YL, Pasternak GW, et al. A heroin addiction severity-associated intronic single nucleotide polymorphism modulates alternative pre-mRNA splicing of the mu opioid receptor gene OPRM1 via hnRNPH interactions. J. Neurosci. 2014; 34:11048–11066. [PubMed: 25122903]

Zhang C, Frias MA, Mele A, Ruggiu M, Eom T, Marney CB, Wang H, Licatalosi DD, Fak JJ, Darnell RB. Integrative modeling defines the Nova splicing-regulatory network and its combinatorial controls. Science. 2010; 329:439–443. [PubMed: 20558669]

Zhang P, Casaday-Potts R, Precht P, Jiang H, Liu Y, Pazin MJ, Mattson MP. Nontelomeric splice variant of telomere repeat-binding factor 2 maintains neuronal traits by sequestering repressor element 1-silencing transcription factor. Proc. Natl. Acad. Sci. USA. 2011; 108:16434–16439. [PubMed: 21903926]

Zhang P, Furukawa K, Opresko PL, Xu X, Bohr VA, Mattson MP. TRF2 dysfunction elicits DNA damage responses associated with senescence in proliferating neural cells and differentiation of neurons. J. Neurochem. 2006; 97:567–581. [PubMed: 16539655]

Zhang P, Pazin MJ, Schwartz CM, Becker KG, Wersto RP, Dilley CM, Mattson MP. Nontelomeric TRF2-REST interaction modulates neuronal gene silencing and fate of tumor and stem cells. Curr. Biol. 2008; 18:1489–1494. [PubMed: 18818083]

Highlights

- A splice variant of TRF2 with a short exon 7 (TRF2-S) arises during neurogenesis
- HNRNPH1/H2 binds *Trf2* exon 7 and represses splicing into TRF2-S
- During neurogenesis, HNRNPH1/H2 levels decline while TRF2-S levels increase
- Silencing HNRNPH1/H2 elevates TRF2-S and promotes neurogenesis

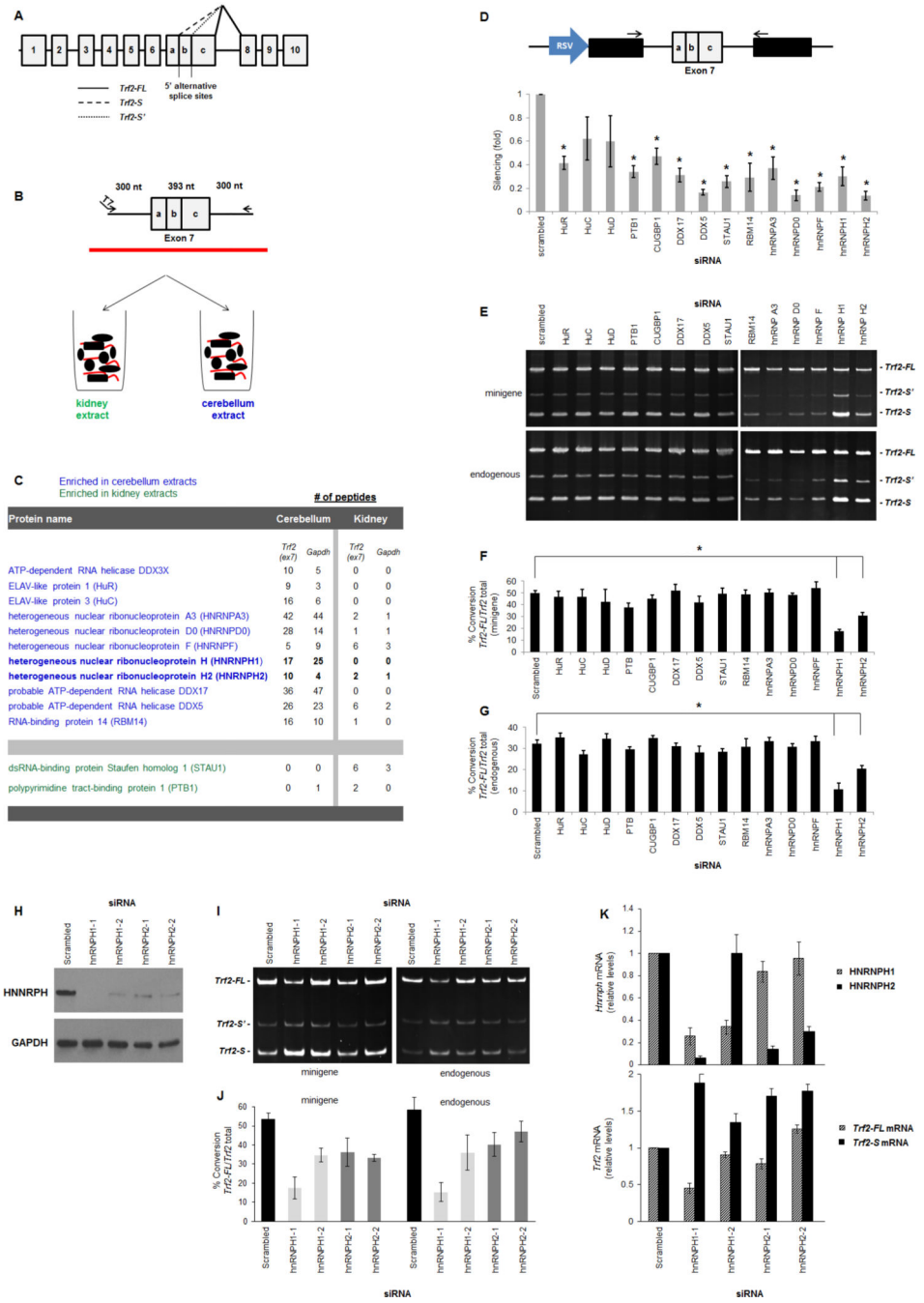

Figure 1. Identification of proteins binding to and regulating *Trf2* exon 7 splicing

(A) Schematic representation of the *Trf2* gene and the isoforms produced by alternative splicing of exon 7. Boxes indicate exons and straight lines introns. Exon 7 contains 3 segments; inclusion of all segments produces *Trf2-FL* mRNA, while use of 5' alternative splice site produces *Trf2-S* and *Trf2-S'* mRNAs. **(B)** Scheme of exon 7 and 300-nt flanking intronic sequences used in *in vitro* binding assay with biotinylated RNA (red line). Primers are indicated with arrows; the T7 promoter sequence was used to generate a PCR product suitable for *in vitro* transcription. Incubations were carried out with kidney and cerebellum

extracts. **(C)** After pulldown using streptavidin beads, interacting proteins were size-fractionated by SDS-PAGE and analyzed by mass spectrometry. Among the proteins in the pulldown materials, those selectively enriched in cerebellum (*top*) and kidney (*bottom*), along with the number of peptides found by mass spec analysis, are listed. Biotinylated rat *Gapdh* 3'UTR RNA was included as negative control. **(D)** Schematic of the minigene used in the splicing assay. Exon 7 was cloned into a vector containing heterologous sequences for introns and exons (Singh and Cooper, 2006). *Arrows*, primers used to amplify the spliced segment. *Graph*, 48 h after transfection of each siRNA, RBP silencing was determined by the levels of RBP mRNA remaining compared with the scrambled siRNA transfection group. **(E–G)** Acrylamide gels showing semi-quantitative PCR products from the minigene (E, *top*) or endogenous gene (E, *bottom*); each lane represents a different cell population in which a given RBP identified by mass spectrometry was silenced using siRNA; control cells transfected with scrambled siRNA were included. The levels of conversion (*Trf2-FL* RNA relative to total *Trf2* RNA bands) from the minigene (F) or the endogenous gene (G) were calculated. **(H–J)** 48 h after transfecting PC12 cells with two different siRNAs for each HNRNPH or scrambled siRNA, Western blot analysis was used to assess HNRNPH levels (H), and acrylamide gels were used to visualize semi-quantitative PCR products from the minigene (I, *left*) or endogenous gene (I, *right*). Control cells were transfected with scrambled siRNA. The levels of conversion (*Trf2-FL* band relative to total *Trf2* bands) from the minigene or the endogenous gene were calculated (J). **(K)** 48 h after transfecting PC12 cells with two different siRNAs for each HNRNPH or scrambled siRNA, RT-qPCR analysis was performed to measure the levels of *Hnrnph1, Hnrnph2, Trf2-S* and *Trf2-FL* mRNAs; Western blot analysis was performed to assess the levels of HNRNPH and loading control GAPDH. In (D–G,J,K), the data represent the means +S.E.M from at least three experiments; *, $p<0.05$.

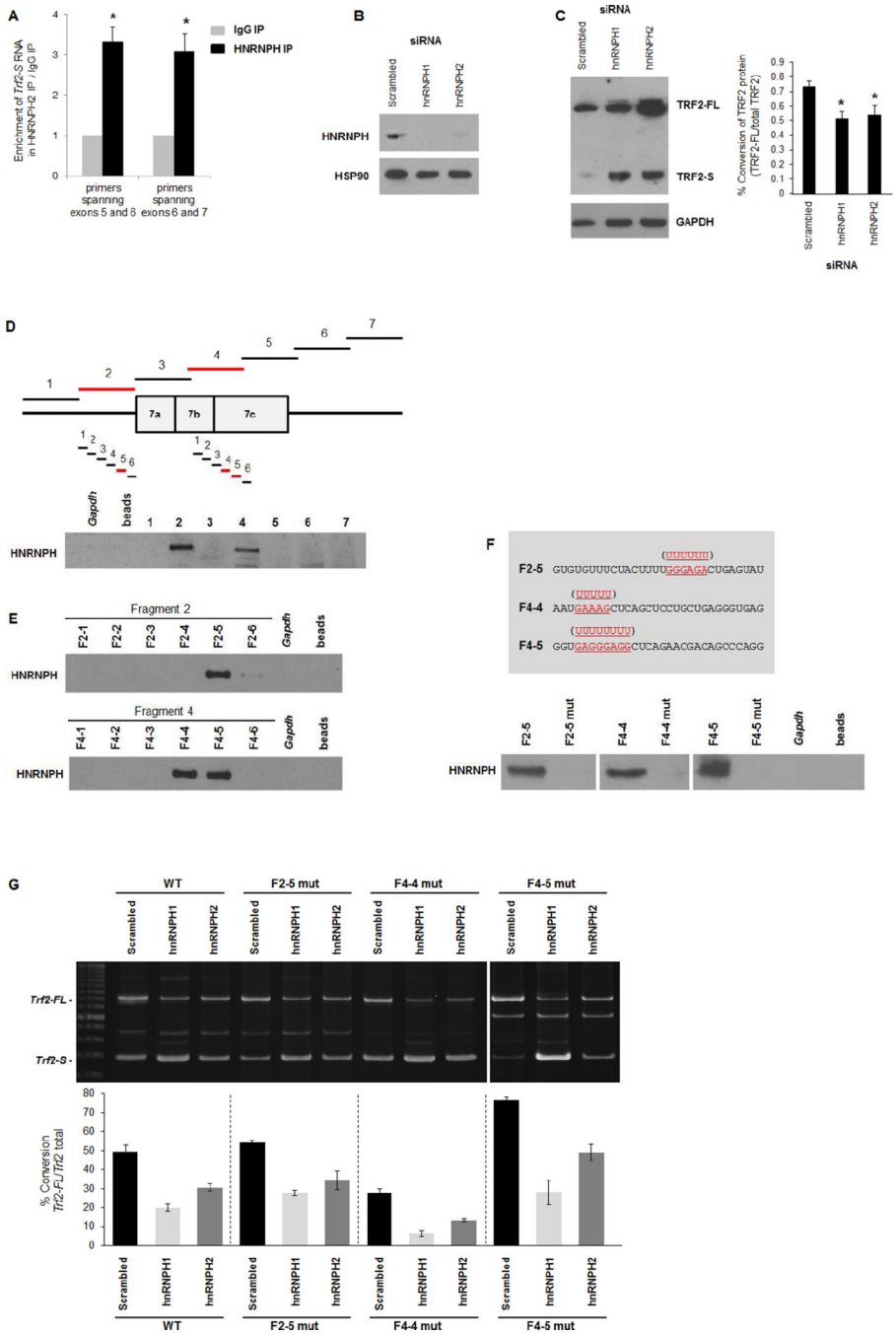

Figure 2. HNRNPH proteins bind to exon 7 and regulate *Trf2* exon 7 splicing

(A) RIP analysis to measure the enrichment of *Trf2* mRNA [and input control *Tbp* mRNA (TATA-binding protein)] by RT-qPCR analysis in HNRNPH IP relative to IgG IP. Two different sets of primers were used, one spanning exons 5 and 6 (*left*) the other spanning exons 6 and 7 (*right*). **(B,C)** 48 h after transfecting PC12 cells with scrambled, HNRNPH1 or HNRNPH2 siRNAs, Western blot analysis was used to analyze the levels of HNRNPH (B) and TRF2-FL and TRF2-S (C). Anti-HNRNPH recognized both isoforms; the levels of GAPDH were assessed to monitor loading; *graph* (C), ratios of TRF2-FL to total TRF2 after

quantification by densitometry. **(D)** Exon 7 and flanking intronic sequences used to identify the binding sites of HNRNPH (*top*). Large (150-nt long) fragments were tested first (horizontal lines above the schematic). Smaller (30-nt long) subfragments of fragments 2 and 4 are shown. Red fragments indicate binding. After incubation, Western blot analysis was used to identify the biotinylated RNAs associating with HNRNPH (fragments 2 and 4). **(E)** Similar biotin pulldown analysis using subfragments 1–6 from fragments 2 and 4. **(F)** Sequences of the three putative sites binding to HNRNPH. The red underlined sequences indicate the potential binding sites that were mutated into Us. *Lower*, biotin pulldown analysis of HNRNPH binding subfragments F2-5, F4-5 and F4-5 and corresponding mutants. In D-F, biotinylated *Gapdh* 3'UTR and beads only were used as negative controls. **(G)** Acrylamide gels showing the PCR products from the minigene (WT) and minigenes each contacting a mutated binding site (F2–5 mut, F4-4 mut, F4-5 mut). Each minigene was assayed in cells transfected with scrambled siRNA, HNRNPH1 siRNA or HNRNPH2 siRNA. *Graph*, conversion ratios (*Trf2-FL* mRNA relative to total *Trf2* mRNA) from the minigene. Data represent the means +S.E.M from at least three experiments; *, $p<0.05$.

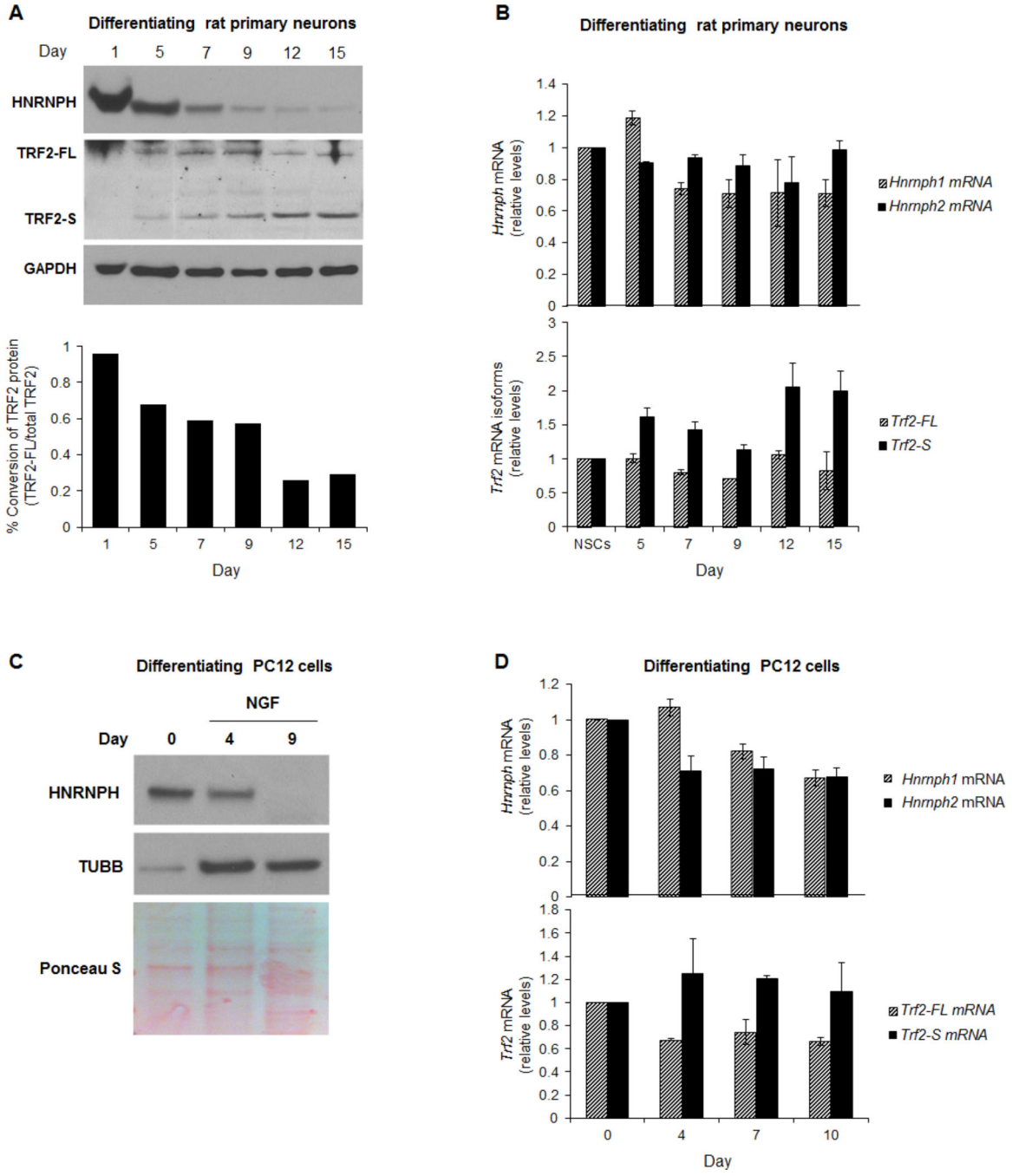

Figure 3. HNRNPH levels decline during neuronal differentiation

(A,B) Primary rat cortical neurons from embryonic day 14 were cultured in differentiation media; at the times indicated, Western blot analysis to monitor the levels of HNRNPH2, TRF2-FL, TRF2-S, and loading control GAPDH. *Graph*, % conversion (ratios of TRF2-FL relative to total TRF2) during differentiation (A). RT-qPCR analysis to measure the levels of *Hnrnph1, Hnrnph2, Trf2-S*, and *Trf2-FL* mRNAs in differentiating neurons compared to undifferentiated neurons (neural stem cells). **(C,D)** During differentiation of PC12 cells in the presence of NGF, the levels of HNRNPH and loading control TUBB (β-Tubulin) were

measured by Western blot analysis; since TUBB levels changed, a photograph of the Western blot membrane stained with Ponceau S red was included (C). RT-qPCR analysis of the levels of *Hnrnph1, Hnrnph2, Trf2-S*, and *Trf2-FL* mRNAs compared to untreated cells (D). In (B, D), data represent the means +S.E.M from at least three experiments.

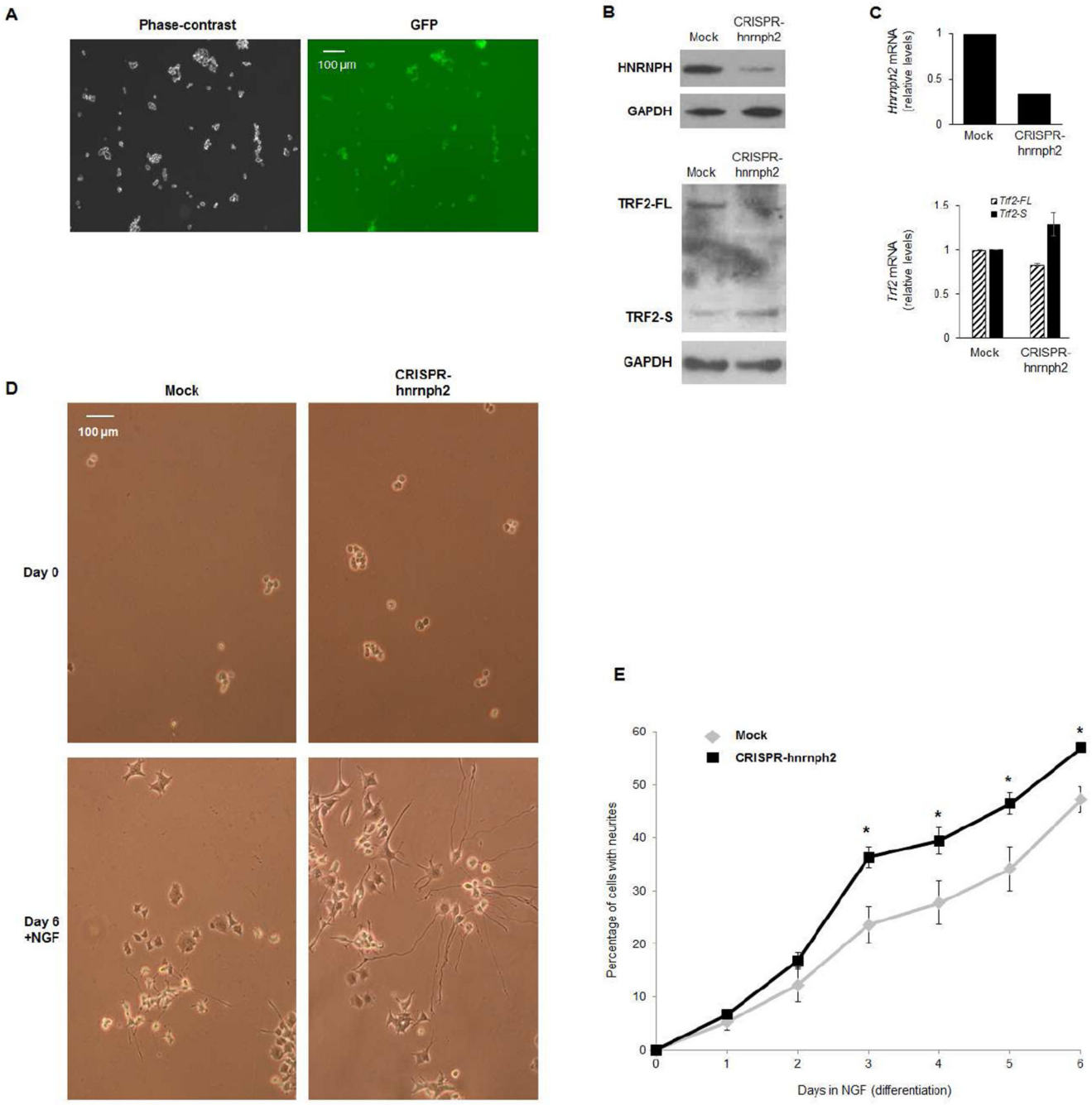

Figure 4. Inhibiting HNRNPH2 promotes neuronal differentiation of PC12 cells

(A) Phase-contrast and fluorescence (GFP) micrographs of pooled PC12 populations with CRISPR/Cas9 directed at HNRNPH2; virtually 100% of cells expressed GFP. **(B, C)** In uninfected or CRISPR-virus-infected cells described in (A), Western blot analysis was used to measure the levels of HNRNPH2, loading control GAPDH, TRF2-FL and TRF2-S (B), and RT-qPCR analysis was used to measure the levels of *Hnrnph2, Trf2-FL*, and *Trf2-S* mRNAs (C). **(D)** Representative micrographs of uninfected and CRISPR-HNRNPH2 virus-infected PC12 cells shown in (A) before and after differentiation (NGF for 6 days). **(E)**

Graph represents the percentage of differentiated PC12 cells (cells with at least one neurite extension that was at least twice as long as the diameter of the cell body). Data represent the means +S.E.M from four experiments; *, $p<0.05$.